Evaluation of a Unidirectional Three-Phase Rectifier based on the Third Harmonic Injection Concept in Comparison to a VIENNA Rectifier

M. Makoschitz, M. Hartmann*, H. Ertl

Vienna University of Technology, Institute of Energy Systems and Electrical Drives,
Power Electronics Section, Gusshausstrasse 27-29, A-1040 Wien, Vienna, Austria
*) Schneider Electric Power Drives GmbH, Vienna, Austria
Email: markus.makoschitz@tuwien.ac.at

Abstract

One of the most attractive rectification circuit for three-phase AC-to-DC conversion is the very well known three-phase diode (B6) bridge rectifier. Simplicity of circuit and design, high efficiency as well as robustness and cost-efficiency are major beneficial outcomes of this type of rectifier.
For applications which require high input current quality (low THD and a high power factor) active three-phase rectifiers (e.g. VIENNA rectifier) have to be used which in general are dedicated systems fully replacing the passive rectifier.
For specific applications which do not require a controlled output voltage (e.g., AC drives), however, a concept seems to be attractive, which opens the opportunity to optionally extend an existing B6 rectifier to a low harmonic input stage. In order to emphasize additional benefits and drawbacks of the optional third harmonic injection circuit (employing two half-bridge branches) compared to an active unidirectional rectifier commonly used in industry (e.g. the VIENNA rectifier), this work is engaged in an opposed comparison of different performance indices as system efficiency, switching/conduction losses, rated inductor power etc.

1. Introduction

The passive three-phase diode bridge rectifier (B6) is an attractive solution if a highly efficient, robust and simple low-cost rectification circuit is required which is operable at a fixed output voltage level (dependent on mains input voltage levels). Major field of interests for such a rectifier are e.g. AC drives, switch-mode power supplies, charging stations for electric vehicles etc. The B6 (as indicated in **Fig. 1**) mainly consists of a three-phase diode bridge (D_1-D_6), a smoothing inductor (L_{DC} - mainly located at the DC-side) and an electrolytic capacitor output stage (C_{o}). Due to the rather few component count and the purely passive implementation of the circuit, it is indeed a very cost effective mains input stage. The electrical characteristics of the topology are however limited by a power factor of $0.9 \ldots 0.95$ and a rather high harmonic input current distortion ($\mathrm{THD_i}$) of up to $48\,\%$ (nominal load operation).
If a low harmonic circuit on the other hand is required (e.g. by regulation) without fully redesigning the passive bridge an optional active current shaping concept may be of interest which is formally known as "third harmonic injection" (THI) principle (discussed in [1]). The idea is to separately design an active circuit which is fitting the electrical characteristics of the already existing passive three-phase rectifier and acts as optional upgrade for the B6 bridge. The equipped converter system offers an adequate solution to provide unity power factor ($\lambda = 1$) and elim-

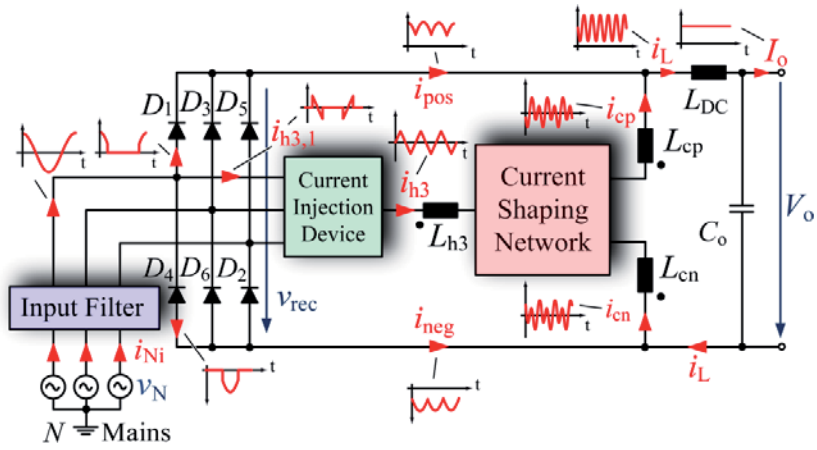

Fig. 1: Basic concept of the third harmonic injection principle. The optional active upgrade consists of a "current shaping network" (CSN) and a current injection device (CID) which are responsible for obtaining properly shaped sinusoidal mains currents i_{Ni}.

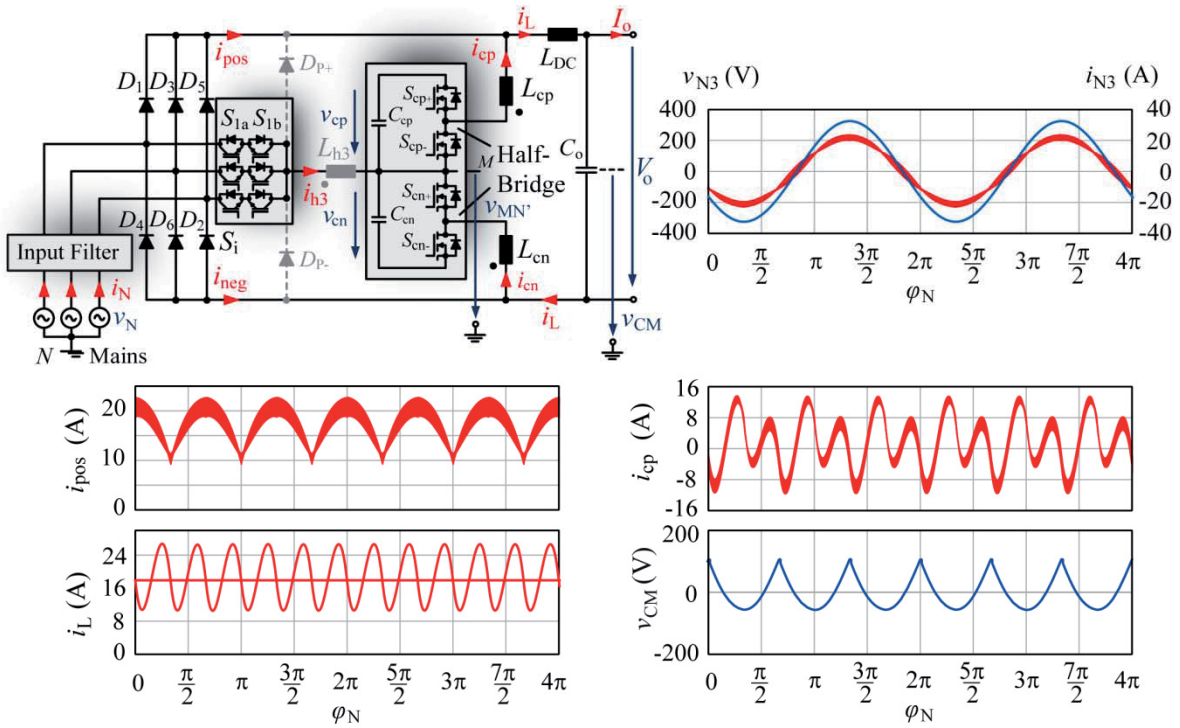

Fig. 2: Third harmonic injection concept employing 2 half-bridges branches as proposed in [2,3] and appropriate simulated most relevant voltage and current signals v_{N3}, i_{N3}, i_{pos}, i_{cp}, i_L, v_{CM} and I_o for $10\,\mathrm{kW}$ rated output power.

inates low harmonic currents at the AC-side input ($\mathrm{THD_i} < 5\,\%$) for a wide power range.

The optional active power electronics network, is going to be connected to the passive bridge at five points of the rectifier, which are typically accessible. The upgrade generates currents i_{cp} and i_{cn} which are going to be injected into the positive and negative bus bar of the passive bridge (current shaping network). These currents are required in order to compensate the unfavorable $300\,\mathrm{Hz}$ harmonic current of the LC output filter current i_L and furthermore form $150\,\mathrm{Hz}$ sinusoidal wave shapes. Purely sinusoidal input currents are finally achieved by filling up the naturally (due to passive rectification) evoked zero current gaps by a third harmonic current i_{h3} which is going to be injected (current injection device) into the appropriate mains phase.

Several active circuits which are able to fulfill these requirements have been proposed and presented already (cf., [2]).

2. Pertained Competitive Rectifiers

One feasible implementation of the third harmonic injection rectifier is depicted in **Fig. 2**. The black box which was labeled as "current shaping network" (CSN) has e.g. been replaced by a series connection of two half-bridge legs. Each half-bridge can either consist of 2 SiC - MOSFETs (or IGBTs). The DC - link of the cell is defined by $600\,\mathrm{V}$ for proper operation ($M = 3V_{\mathrm{Npk}}/V_c = 0.8125$) of the circuit, which consequently leads to $900\,\mathrm{V}/1200\,\mathrm{V}$ SiC devices. The current injection device (3 bidirectional switches) which forms the interconnection between AC-side input and DC-side current shaping network can be implemented by **(i)** back-to-back connected IGBTs/SiC-MOSFETs (reverse conducting IGBTs applicable and only 1 DC/DC converter required for 1 bidirectional switch gate drive), **(ii)** reverse blocking IGBTs, **(iii)** one active switch (e.g. IGBT/MOSFET) and 4 diodes or **(iv)** 2 diodes and 2 IGBTs/MOSFETs.

In-between CSN and CID an optional third inductor L_{h3} is considered in order to further improve the input current quality of system (as discussed in [3]). A switching frequency of $72\,\mathrm{kHz}$ finally leads to inductance values for L_{cp}, L_{cn} and L_{h3} of $190\,\mu\mathrm{H}$ (for $10\mathrm{kW}$ nominal output power).

Alternatively to the proposed rectifier concept, one of the most attractive PFC circuits for unidirectional power flow, is the ***VIENNA rectifier*** (e.g. [4-6]). There are different topologies available. The VIENNA rectifier depicted in **Fig. 3** has a very low number of active and passive switches and is, therefore,

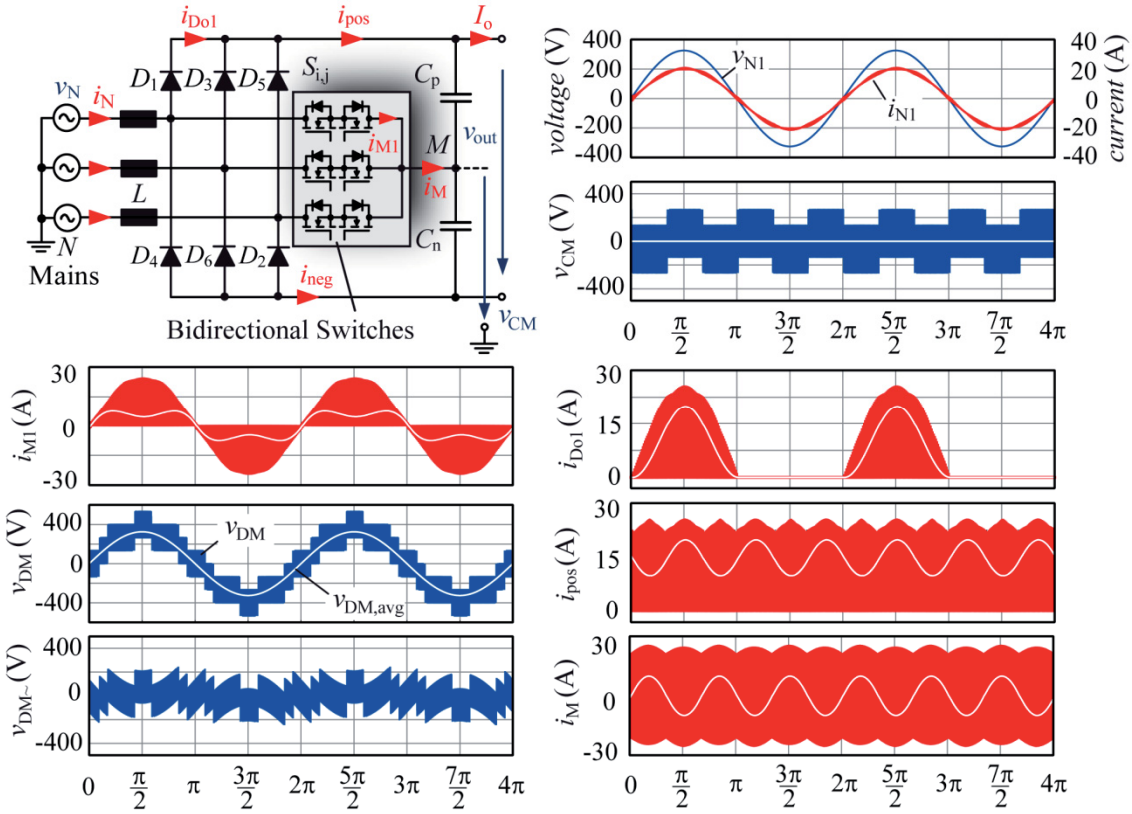

Fig. 3: VIENNA rectifier with 6 600 V MOSFETs which form the interconnection between AC-side and output capacitors midpoint M and diode bridge (typically implemented fast recovery diodes).

going to serve as competitive partner for this investigation. It has to be noted that a comparison of these two active rectifiers should NOT identify a superior concept (which is indeed not possible due to completely different attributes of both rectifiers). The investigation should merely reveal benefits and drawbacks of the THI circuit by comparing the upgradeable rectifier to a today well established industrial standard PFC concept.

3. Benchmarking Specifications

A reliable comparison between the two active systems shall allow an advanced benchmarking of the THI rectifier. Therefore, different performance indices (which are going to be used for this comparison) are introduced, listed and shortly described in the following.

A. Diode/MOSFET VA-Ratings: The VA-ratings of a switching component is defined by multiplication of maximum blocking voltage and peak current of the appropriate semiconductor. This factor hence gives a prediction of the relative maximum stress of diodes (μ_D^{-1}) and transistors (μ_S^{-1}) in a power electronics circuit and can hence be determined by

$$\mu_S^{-1} = \frac{\sum_n v_{S,max,n} i_{S,max,n}}{P_o} \quad \text{and} \quad \mu_D^{-1} = \frac{\sum_n v_{D,max,n} i_{D,max,n}}{P_o}.$$

B. Rated Inductor Power/Capacitor Current Stress: Two major performance aspects in order to classify inductors and capacitors in an electrical way, are to introduce a rated inductor power index ρ_L and a normalized capacitive current stress equivalent ρ_C of all implemented inductors and capacitor stages within the converter system.

$$\rho_L = \frac{\sum_n I_{L,n} \Delta I_{L,pkpk,n} L_{c,n} f_s}{P_o}, \qquad \rho_C = \frac{\sum_n I_{C,rms,n}}{I_o}.$$

C. Inverse Power Density of Inductors: Besides electrical characteristics of inductors, also a volume dependent design might be of interest for the final implementation of the total rectifier system. Therefore, the power density of the implemented inductors is selected as promising benchmark indexing.

ISBN 978-3-8007-4186-1

$$\varepsilon_{\mathrm{L}}^{-1} = \frac{\sum_{\mathrm{n}} V_{\mathrm{L,n}}}{P_{\mathrm{o}}}$$

D. Switching Losses of Semiconductors: Furthermore, the switching losses of all impaired components are compared to each other with respect to the total output power P_{o}. τ_{p} can be qualitatively determined by

$$\tau_{\mathrm{p}} = \frac{\sum_{\mathrm{n}} I_{\mathrm{S,avg,n}} V_{\mathrm{S,n}}}{P_{\mathrm{o}}}$$

E. Conduction Losses of Diodes and Switches: Conduction losses of switches and diodes can be opposed by evaluation of averaged and rms current values related to the output current (cf., [7]).

$$\tau_{\mathrm{c}} = \frac{\sum_{\mathrm{n}} I_{\mathrm{S,rms,n}}}{I_{\mathrm{o}}}, \qquad \delta_{\mathrm{c}} = \frac{\sum_{\mathrm{n}} I_{\mathrm{D,avg/rms,n}}}{I_{\mathrm{o}}}.$$

F. System Efficiency: Finally the performance of the total system is going to be determined by comparing total losses of both active systems.

$$1 - \eta = \frac{P_{\mathrm{in}} - P_{\mathrm{o}}}{P_{\mathrm{in}}}.$$

4. Comparative Values - THI

In this section, the previously described performance indices are now going to be derived analytically. The VA-ratings of the implemented semiconductor is the first parameter of interest in this evaluation. The THI rectifier diodes ($D_{1\text{-}6}$) are stressed with a maximum blocking voltage which is dependent according to the peak line-to-line voltage situation ($v_{\mathrm{D,max}} = \sqrt{2}\,V_{\mathrm{LL}}$) and a maximum current which is equivalent to I_{Npk}. The diodes of one bidirectional switch, however, obtain their maximum while the two remaining bidirectional switches initiate the current commutation of i_{h3}. This commutation however takes place before the applied line-to-line voltage attains its maximum value. The maximum blocking voltage of the diodes (and thus also transistors) of bidirectional switches is hence defined by $3V_{\mathrm{Npk}}/2$, and the maximum current is defined according to i_{h3} (whose peak value is defined by $I_{\mathrm{Npk}}/2$).
The switches of each half-bridge are stressed with the peak current of injection currents i_{cp}, i_{cn} and the DC voltage of C_{cp}, C_{cn}, respectively. The VA ratings of switches and diodes hence lead to

$$\mu_{\mathrm{S}}^{-1} = \frac{9\hat{V}_{\mathrm{N}}\hat{I}_{\mathrm{N}} + 16V_{\mathrm{c}}\hat{I}_{\mathrm{cp}}}{4P_{\mathrm{o}}} \qquad \mu_{\mathrm{D}}^{-1} = \frac{6\hat{V}_{\mathrm{N}}\hat{I}_{\mathrm{N}}\left(8\sqrt{3}+3\right)}{8P_{\mathrm{o}}}.$$

In order to evaluate the current stress of capacitors, 3 different capacitor banks have to be evaluated (C_{cp}, C_{cn} and C_{o}). C_{o} is characterized by $I_{\mathrm{L,ac,pk}}/2$. Current stress of half-bridge capacitors C_{cp}, C_{cn}, can only be determined numerically and result in $3.6\,\mathrm{A_{rms}}$ for an output power of $10\,\mathrm{kW}$. The normalized capacitive current stress ρ_{C} of all implemented capacitors of the THI rectifier then results in

$$\rho_{\mathrm{C}} = \frac{\hat{I}_{\mathrm{L,ac}} + 2\sqrt{2}I_{\mathrm{ccp}}}{\sqrt{2}I_{\mathrm{o}}}, \quad \text{with} \quad \hat{I}_{\mathrm{L,ac}} = \frac{\sqrt{3}\hat{V}_{\mathrm{N}}}{\omega_{\mathrm{N}}L_{\mathrm{DC}}}\left(\sin\left(\arccos\left(\frac{3}{\pi}\right)\right) - \frac{3}{\pi}\arccos\left(\frac{3}{\pi}\right)\right).$$

The rated inductor power (of the appropriate implemented chokes L_{cp}, L_{cn}, L_{h3} and L_{DC}) is dependent on current rms values I_{cp}, I_{cn}, I_{h3}, I_{L}, and the appropriate maximum peak-to-peak current ripples ΔI_{cp}, ΔI_{cn}, ΔI_{h3}, ΔI_{L}, at the operated frequencies f_{s}, $6f_{\mathrm{N}}$. The required appropriate parameters are defined by

$$I_{\mathrm{cp/n}} = \hat{I}_{\mathrm{N}}\sqrt{\frac{2\pi^3 - 24\pi + 9\sqrt{3}}{24\pi} + \left(\frac{\hat{I}_{\mathrm{L,ac}}}{\sqrt{2}\hat{I}_{\mathrm{N}}}\right)^2}, \qquad I_{\mathrm{h3}} = \frac{\hat{I}_{\mathrm{N}}}{2}\sqrt{\frac{2\pi - 3\sqrt{3}}{\pi}}, \qquad I_{\mathrm{L}} = \frac{\hat{I}_{\mathrm{N}}}{2}\sqrt{\frac{2\pi^2}{3} + 2\left(\frac{\hat{I}_{\mathrm{L,ac}}}{\hat{I}_{\mathrm{N}}}\right)^2},$$

$$\Delta I_{\mathrm{cp/n}} = \frac{2MV_{\mathrm{c}}(1-M)}{3f_s L_{\mathrm{cp/n}}}, \qquad \Delta I_{\mathrm{h3}} = \frac{V_{\mathrm{c}}M}{3\sqrt{3}f_s L_{\mathrm{cp/n,h3}}}, \qquad \Delta I_{\mathrm{L}} = 2\hat{I}_{\mathrm{L,ac}}.$$

The rated inductor power hence calculates to

$$\rho_{\mathrm{L}} = \frac{2I_{\mathrm{cp/n}}\Delta I_{\mathrm{cp/n}}L_{\mathrm{cp/,n}}f_{\mathrm{s}} + I_{\mathrm{h3}}\Delta I_{\mathrm{h3}}L_{\mathrm{h3}}f_{\mathrm{s}} + 6I_{\mathrm{L}}\Delta I_{\mathrm{L}}L_{\mathrm{DC}}f_{\mathrm{N}}}{P_{\mathrm{o}}}.$$

In order to identify conduction losses of switches (rms) and diodes (avg), the current stress of corresponding components is required which can be finally determined by

$$I_{\mathrm{D1\text{-}6,avg}} = \frac{\sqrt{3}\hat{I}_{\mathrm{N}}}{2\pi}, \qquad I_{\mathrm{Diab,avg}} = \frac{\hat{I}_{\mathrm{N}}}{2\pi}\left(2-\sqrt{3}\right), \qquad I_{\mathrm{Siab,rms}} = \hat{I}_{\mathrm{N}}\sqrt{\frac{2\pi - 3\sqrt{3}}{24\pi}}.$$

ISBN 978-3-8007-4186-1

The current stress of both half-bridge semiconductors can again only be calculated numerically and eventually result in $3.6\,\mathrm{A_{rms}}$ and $5\,\mathrm{A_{rms}}$ for the positive (S_+) and negative switch (S_-) of one half-bridge, respectively ($10\,\mathrm{kW}$ nominal load operation). If all derived characteristics are considered, conduction losses of both, diodes and transistors thus result in

$$\delta_\mathrm{c} = \frac{6}{\pi}\frac{\hat{I}_\mathrm{N}}{I_\mathrm{o}}, \qquad \tau_\mathrm{c} = \frac{3\hat{I}_\mathrm{N}\sqrt{2\pi - 3\sqrt{3}} + 2\sqrt{6\pi}\,(I_{\mathrm{S}+} + I_{\mathrm{S}-})}{\sqrt{6\pi}I_\mathrm{o}}.$$

The switching losses of the system can be "qualitatively" determined by utilizing the averaged pulsed current of the each switch (assuming linear dependency of the switching losses on the switched current) and applied drain source voltage (during the off state of the transistor). It has to be noted, that the bidirectional switches of the THI rectifier are only turned on and off twice during one mains period. Switching losses of these device are hence negligibly small. The only devices which are operated with switching frequency f_s are the half-bridge semiconductors (S_+, S_-). The averaged values of these components can be determined numerically and lead to $0\,\mathrm{A_{avg}}$ and $1.6\,\mathrm{A_{avg}}$, respectively. τ_p therefore can be assessed and yields

$$\tau_\mathrm{p} = \frac{2I_{\mathrm{S}-}V_\mathrm{c}}{P_\mathrm{o}}.$$

The coils of the injection cell are designed such to allow a maximum ripple of $20\,\%\,I_\mathrm{Npk}$ which results in an inductance value of $\sim 190\,\mu\mathrm{H}$ for the required power level of $10\mathrm{kW}$. The implemented inductor (stacked core assembly) leads to a core volume of $0.074\,\mathrm{dm^3}$ for each inductor (stacked core: 2xT184-14, windings: 59). The necessary passive three-phase rectifier choke is a $300\,\mathrm{Hz}$ inductor and hence considerably larger than the injection coils (as it is typically designed for a maximum input current $\mathrm{THD_i}$ value of $48\,\%$ for B6 standalone operation). The volume of the implemented inductor results in $0.57\,\mathrm{dm^3}$ (not optimized). The reciprocal power density of all inductors of the THI rectifier is defined by

$$\varepsilon_\mathrm{L}^{-1} = \frac{3V_\mathrm{L} + V_\mathrm{LDC}}{P_\mathrm{o}}$$

The efficiency of the total system was calculated to be $\sim 98\,\%$ and $97.8\,\%$ has been measured ($10\,\mathrm{kW}/72\,\mathrm{kHz}$ prototype) for a nominal load of $10\,\mathrm{kW}$. The total losses of the system can therefore be assessed and result in $1\text{-}\eta = 2.2\,\%$.

5. Comparative Values - VIENNA

The maximum blocking voltage of the VIENNA rectifier diodes ($D_{1\text{-}6}$) is dependent on the required (and controllable) output voltage V_o. The maximum diode current is (as for the THI rectifier topology) the peak mains input current I_Npk. Blocking voltages levels of each diode of the bidirectional switches only have to withstand $V_\mathrm{o}/2$. Similar assumptions as discussed for diodes of the bidirectional switches also apply for appropriate MOSFETs. The VA-ratings of implemented switches therefore results in

$$\mu_\mathrm{D}^{-1} = \frac{9V_\mathrm{o}\hat{I}_\mathrm{N}}{P_\mathrm{o}} \qquad \text{and} \qquad \mu_\mathrm{S}^{-1} = \frac{3V_\mathrm{o}\hat{I}_\mathrm{N}}{P_\mathrm{o}}.$$

The capacitor current stress of the VIENNA rectifier output capacitors (both connected to the midpoint M) can be evaluated in an analytical form. The normalized capacitive current stress ρ_C of the required output capacitor stage of the rectifier is therefore defined by

$$\rho_\mathrm{C} = 2\frac{\hat{I}_\mathrm{N}}{I_\mathrm{o}}\sqrt{\frac{5\sqrt{3}M}{4\pi} - \frac{9M^2}{16}} \quad \text{with} \quad M = \frac{2\hat{V}_\mathrm{N}}{V_\mathrm{o}}.$$

In order to characterize the rated inductor power of the VIENNA rectifier, it is assumed that the maximum current ripple does appear at $\varphi_\mathrm{N} = 0°$, which is valid for a modulation index $M > 0.85$ ($V_\mathrm{o} < 760\,\mathrm{V}$). For smaller values of M, $\Delta I_\mathrm{L,max}$ is located at $\varphi_\mathrm{N} = 30\,°$ which is neglected for the comparison at hand. The inductor rms current is defined by the input current rms and results in $I_\mathrm{L,rms} = I_\mathrm{N,rms}$. The rated inductor power then leads to a ρ_L of

$$\rho_\mathrm{L} = \frac{3}{4\sqrt{2}}\frac{\hat{I}_\mathrm{N}V_\mathrm{o}}{P_\mathrm{o}}\left(\frac{8}{3}M - M^2 - \frac{4}{3}\right).$$

The boost inductors of an $800\mathrm{V}$ VIENNA, are implemented as Schott 193 type coils. The total volume of all 3 chokes results in $0.285\,\mathrm{dm^3}$, which leads to an reciprocal power density of $0.029\,\mathrm{dm^3/kW}$.

ISBN 978-3-8007-4186-1

In a next step the conduction losses of transistors and diodes are going to be calculated. The transistor conduction losses are represented by the rms value of its drawn current for one mains period. The diodes conduction losses are, however, characterized by its averaged current values. The evaluated values of transistors and diodes conduction losses eventually result in

$$\tau_{\mathrm{c}} = 6\frac{\hat{I}_{\mathrm{N}}}{I_{\mathrm{o}}}\sqrt{\frac{1}{4}-\frac{2M}{3\pi}} \qquad \text{and} \qquad \delta_{\mathrm{c}} = \frac{6}{\pi}\frac{\hat{I}_{\mathrm{N}}}{I_{\mathrm{o}}}.$$

The switching losses can be again "qualitatively" identified by the averaged current of the appropriate semiconductor. The switching losses of $S_{1\text{-}6}$ hence result in

$$\tau_{\mathrm{p}} = 3\frac{\hat{I}_{\mathrm{N}}V_{\mathrm{o}}}{P_{\mathrm{o}}}\left(\frac{1}{\pi}-\frac{M}{4}\right).$$

The efficiency of the VIENNA rectifier for $800\,\mathrm{V}$ output voltage was documented in [7] and has been evaluated to be $97.3\,\%$.

6. Comparison of Results

Results of the performance evaluation for both rectifiers (implemented THI prototype cf., **Fig. 4(a)**) are going to be summarized in two different "radar diagrams" (VIENNA rectifier with $650\,\mathrm{V}$ and $800\,\mathrm{V}$ regulated output voltage V_{o}) as depicted in **Fig. 4(b)** and e.g. used in [8]. The output voltage levels of the VIENNA rectifier are chosen such to provide comparison values for a minimum achievable output voltage ($650\,\mathrm{V}$- if midpoint voltage control is not considered) and one commonly used output voltage level ($800\,\mathrm{V}$) of the VIENNA rectifier. It is however important to bear in mind that the THI rectifier is characterized by a fixed output voltage according to the mains voltage situation ($537\,\mathrm{V}$). The variation of the output voltage of the VIENNA rectifier should therefore only illustrate the modification of the selected parameters of the VIENNA in comparison to the THI rectifier. Predefined specifications of the rectifier systems which are used for benchmarking are given in **TABLE I**. Results of the calculated performance indices are listed in **TABLE II**. The performance parameters are chosen such, that a smaller value emphasizes a good system behaviour. One conspicuous feature of the THI rectifier is the small values of conduction and switching losses of diodes and transistors. This is mainly evoked due to the fact that the additional active converter stage only has to transfer a small amount of output power ($\sim 6\,\%$) and process approximately $17\,\%$ of reactive power. Additionally, it has to be considered that, although rated inductor power of both circuits seem to be of similar value, the implemented inductor volume of the THI rectifier is definitely higher than that of a VIENNA rectifier. This underlies the fact, that the THI rectifier system requires an additional 4$^{\mathrm{th}}$ inductor (due to passive rectification). This coil is however electrically characterized by a $300\mathrm{Hz}$ current ripple and its size majorly defined according to the specified $\mathrm{THD_i}$ for B6 standalone operation. Hence, no shrinking due to increased switching frequency is possible for the volume and design of L_{DC}.

Furthermore, as can be read from **TABLE II**, both rectifiers obviously show strong- and weak-points. Drawbacks of the THI rectifier are for example

- the high inductor volume, which is majorly determined due to the $300\mathrm{Hz}$ choke (which belongs to the original passive rectifier),
- the relatively large component count (4 additional switching devices) compared to the VIENNA rectifier (however it has to be noted that 6 switches S_{ij} of the VIENNA rectifier are stressed with switching frequency, but merely 4 switches $S_{\mathrm{cp/n\pm}}$ of the THI rectifier),
- higher complexity of the total system
- no regulation of output voltage V_{o} available (fixed according to mains voltage situation).

On the other hand, however, there are numerous aspects which militates in favor of a THI rectifier system implementation, as e.g.

+ robustness (still operable in B6 standalone mode even if injection cell has to be turned off e.g. due to malfunction) which is primarily attributed to its
+ optional implementation,
+ no high frequency common mode voltage v_{CM} (see **Fig. 2**) at the output of the total system

ISBN 978-3-8007-4186-1

TABLE I: Specifications of the two benchmarked three-phase rectifier systems.

Mains voltage:	$V_{LL} = 400\ V_{rms}$
Mains frequency:	$f_N = 50\ Hz$
Active Rectifier:	VIENNA
THI Rectifier (Shaping circuit):	2 Half-Bridge Branches
THI Rectifier (Injection circuit):	3 Bidirectional Switches
Switching frequency:	$f_s = 72\ kHz.$
THI Cell DC-link voltage:	$V_{cp} = V_{cn} = 600\ V$
THI output voltage (uncontrolled):	$V_o = 537\ V$
VIENNA output voltage (controlled):	$V_o = 650\ V...800\ V$
Output power:	$P_o = 10\ kW$

TABLE II: Results of calculated performance indices of a VIENNA and THI rectifier system.

	VIENNA (650V)	VIENNA (800V)	THI
μ_D^{-1}	11.94	14.7	8.43
μ_S^{-1}	3.98	4.90	4.38
τ_c	1.53	2.71	1.73
τ_p	0.27	0.56	0.2
δ_c	2.53	3.12	2.09
ρ_c	0.94	1.41	0.68
ρ_L	0.24	0.15	0.15
ε_L (dm^3/kW)	0.029	0.016	0.057
$1\text{-}\eta$ (%)	-	2.7	2.2

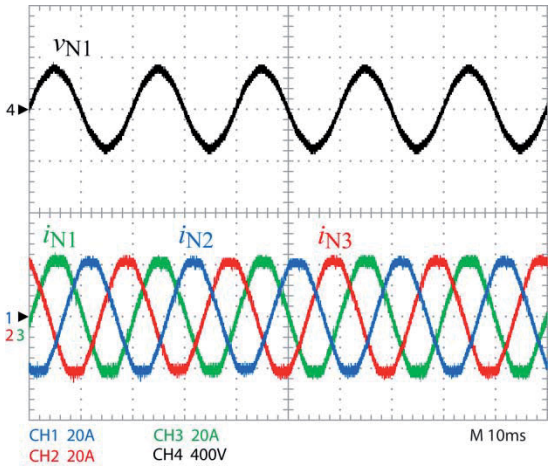

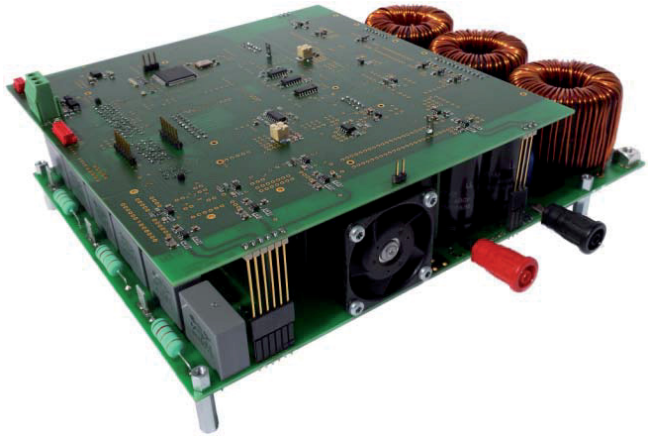

(a)

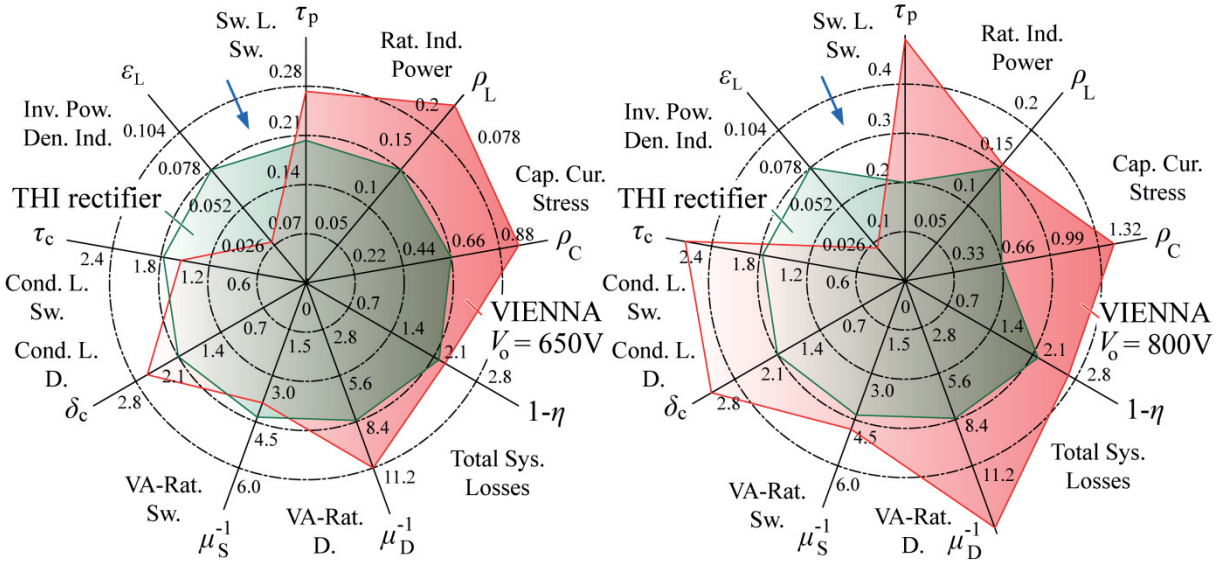

(b)

Fig. 4: (a) Measurement results and constructed laboratory prototype of a 72 kHz/10 kW THI rectifier (cf., [9]) at 10 kW nominal load. The system input is characterized by a power factor of 0.999 and a THD_i between 2-3 % (b) Radar diagram (smaller values characterize a better system behaviour - indicated by blue arrow) consisting of main performance indices comparing a 10 kW VIENNA rectifier with 650V...800V output voltage and a THI rectifier.

ISBN 978-3-8007-4186-1

+ only semiconductors $S_{cp\pm}$ and $S_{cn\pm}$ are stressed with switching frequency.
+ the active upgrade only has to process some fraction of output power

The VIENNA rectifier topology is already widely used in industry and therefore a detailed discussion about pros and cons of this valuable and attractive low harmonic rectifier is not required in this work.

7. Conclusion

Focus of this paper is a comparative evaluation of a selected unidirectional PFC rectifier (VIENNA rectifier) and one specific realization of a rectifier system based on the third harmonic injection principle (2 half-bridge branches). It has once again to be mentioned that, this comparison should merely reveal advantages and drawbacks of the THI circuit by comparing electrical parameters of the upgradeable THI rectifier to an industrial standard PFC concept (VIENNA). It is hence important to notice and/or keep in mind that both topologies originally provide different rectifier attributes (e.g. controllable/no controllable output voltage etc.). Besides benefits and drawbacks also several performance indices are chosen, in order to allow a more reliable characterization and benchmarking of the THI system. The higher circuit complexity of the THI rectifier circuit is compensated by a high efficiency, high robustness and the fact that the THI rectifier shows no high-frequency CM voltage at the DC-output. The circuit does not offer a controlled output voltage, however, the topology reuses the main elements of a passive three-phase rectifier circuit with DC-side located smoothing inductor which allows the extension of an existing passive rectifier circuit to a rectifier circuit with low harmonic input.

Acknowledgement

The authors are very much indebted to the Austrian Research Promotion Agency (FFG) which generously supports the work of the Vienna University of Technology Power Electronics Section (Institute of Energy Systems and Electrical Drives).

References

[1] J. W. Kolar, T. Friedli, "*The Essence of Three-Phase Rectifier Systems*", 33rd Int. IEEE Telecommunications Energy Conference (INTELEC 2011), Amsterdam, Netherlands, Oct. 9-13, pp. 1-27, 2011.

[2] M. Makoschitz, M. Hartmann, H Ertl, "*Topology Survey of DC-side Enhanced Passive Rectifier Circuits for Low-Harmonic Input Currents and Improved Power Factor*", Proceedings of the Conference for Power Electronics, Intelligent Motion, Power Quality (PCIM), Nuernberg, Germany, May 19-21 2015.

[3] M. Makoschitz, M. Hartmann, H. Ertl, R. Fehringer, "*A Passive Three-Phase Rectifier Enhanced by a DC-side High Switching Frequency Add-On SiC-Converter Stage for Unity Power Factor Applications*," in Proceedings of the Conference for Power Electronics, Intelligent Motion, Power Quality (ECCE/EPE), Geneva, Switzerland, September 8-10 2015.

[4] J. W. Kolar, F. Zach, "*A Novel Three-Phase Three-Switch Three-Level PWM Rectifier*," in Proceedings of the Conference for Power Electronics, Intelligent Motion, Power Quality (PCIM), Nuernberg, Germany, June 28-30 1994, pp. 125-138.

[5] J. W. Kolar, H. Ertl, F. Zach, "*Design and experimental investigation of a three-phase high power density high efficiency unity power factor PWM (VIENNA) rectifier employing a novel integrated power semiconductor module*," in Proceedings of the 11th Annual Applied Power Electronics Conference and Exposition (APEC), pp. 514-523, 1996.

[6] M. Hartmann, S. D. Round, H Ertl, J. W. Kolar, "*Digital Current Controller for a 1 MHz, 10kW Three-Phase VIENNA Rectifier*," IEEE Transactions on Power Electronics, pp. 2496 - 2508, 2009.

[7] T. Friedli, M. Hartmann, J. W. Kolar, "*The Essence of Three-Phase PFC Rectifier Systems - Part II*", IEEE Transactions on Power Electronics, Vol. 29, No. 2, February 2014.

[8] T. Soeiro, J. W. Kolar, "*Comparative Evaluation of Bidirectional Buck-Type PFC Converter Systems for Interfacing Residential DC Distribution Systems to the Smart Grid*," Proceedings of the 38th Annual Conference of the IEEE Industrial Electronics Society (IECON 2012), Montreal, Canada, October 25-28, 2012.

[9] M. Makoschitz, M. Hartmann, H Ertl, "*Hardware Implementation and Characterization of a SiC-Based Hybrid Three-Phase Rectifier Employing Third Harmonic Injection*," accepted paper at the 31th Annual Applied Power Electronics Conference and Exposition (APEC), Long Beach, USA, March, 2016.